

Theoretical Investigation on Triagonal Symmetry Copper Trimers: Magneto-Structural Correlation and Spin Frustration

Li-Li Wang,[†] You-Min Sun,[‡] Zhang-Yu Yu,^{†,⊥} Zhong-Nan Qi,[§] and Cheng-Bu Liu^{*,†,||}

Institute of Theoretical Chemistry, Shandong University, Jinan 250100, P. R. China, School of Municipal and Environmental Engineering, Shandong Jianzhu University, Jinan 250101, P. R. China, College of Chemistry and Chemical Engineering, University of Jinan, Jinan 250022, P. R. China, and Key Laboratory of Colloid and Interface Chemistry, Shandong University, Ministry of Education, Jinan, 250100 Shandong, P. R. China

Received: May 17, 2009; Revised Manuscript Received: August 6, 2009

The mechanisms of the magnetic coupling interactions for two trigonal–bipyramid trinuclear Cu(II) complexes $\text{Cu}_3(\mu_3\text{-X})_2(\mu\text{-pz})_3\text{X}_3$ ($\text{X} = \text{Cl}$ and Br , respectively) and three trigonal trinuclear Cu(II) complexes $\text{Cu}_3(\mu_3\text{-X})(\mu\text{-pz})_3\text{Cl}_3$ ($\text{X} = \text{Cl}$, Br , and O) are investigated by the calculations based on density functional theory combined with broken-symmetry approach (DFT-BS). The research on the magneto-structural correlation reveals that the magnetic coupling interaction is sensitive to the Cu–($\mu_3\text{-X}$)–Cu angle. With the Cu–($\mu_3\text{-X}$)–Cu angle changing from 76 to 120°, the magnetic coupling interaction is switched from ferromagnetic to antiferromagnetic. According to the analysis of the molecular orbitals and the variation of the spin-state energies versus the ratio of the magnetic coupling constants, it is found that there exists spin frustration phenomenon in these complexes.

1. Introduction

In the metal-containing proteins, the active sites are often polynuclear transition-metal complexes, and the biological mechanisms in the organisms are always controlled by these active sites.^{1–7} Therefore, to explain the complicated biological phenomena, it is essential to investigate the properties of the polynuclear transition-metal complexes. Compared with the extensive theoretical studies on the binuclear transition-metal complexes,^{8–11} research of the polynuclear systems has been limited.^{12,13} This is because the coupling interaction mechanisms in the polynuclear systems are much more complicated.^{14–16} For example, experimentally, it is found that in the noncollinear polynuclear transition-metal complexes there exists spin frustration phenomenon that results in many interesting magnetic properties.^{17–19} Therefore, recently, more and more researchers have paid attention to the noncollinear polynuclear transition-metal complexes. However, the theoretical elucidation on the magnetic coupling mechanism, especially on the spin frustration phenomenon in the metal-containing proteins, is scanty.

As one simple kind of the polynuclear metal complex, the trigonal trinuclear Cu(II) complexes are attracting much attention for their special phenomena such as spin frustration and their simple structures, which makes the investigation of the mechanism of the magnetic coupling interaction very convenient.^{20,21} Recently, Mezei et al.^{22,23} reported several new $\text{Cu}_3(\mu_3\text{-X})_2(\mu\text{-pz})_3$ complexes and $\text{Cu}_3(\mu_3\text{-X})(\mu\text{-pz})_3$ complexes, which are expected to be models of particulate methane monooxygenase (PMMO). It is found that the magnetic interaction of the $\mu_3\text{-X}$ ($\text{X} = \text{Cl}$ and Br , respectively) doubly bridged trigonal Cu(II) complexes $\text{Cu}_3(\mu_3\text{-X})_2(\mu\text{-pz})_3$ is weak ferromag-

netic coupling, whereas that of the $\mu_3\text{-X}$ singly bridged trigonal Cu(II) complexes $\text{Cu}_3(\mu_3\text{-X})(\mu\text{-pz})_3$ ($\text{X} = \text{O}$ and OH , respectively) is strong antiferromagnetic coupling.^{20,23} From the geometry of these two kinds of compounds, it can be seen that the essential difference is their Cu–($\mu_3\text{-X}$)–Cu angles, which are about 80° in the $\mu_3\text{-X}$ doubly bridged complexes and about 120° in the $\mu_3\text{-X}$ singly bridged complexes. This suggests that the Cu–($\mu_3\text{-X}$)–Cu angles may be the dominant parameters that controlled the magnetic properties of the trigonal trinuclear Cu(II) complexes. Therefore, to elucidate the mechanism of the magnetic coupling interaction and magneto-structure relationship for these systems, we investigate two kinds of compounds mentioned above by density functional theory combined with broken-symmetry approach (DFT-BS) method.

2. Calculated Models

The calculated models A [$\text{Cu}_3(\mu_3\text{-Cl})_2(\mu\text{-pz})_3\text{Cl}_3$] and B [$\text{Cu}_3(\mu_3\text{-Br})_2(\mu\text{-pz})_3\text{Br}_3$] (Figure 1) are predigested from the X-ray crystal geometries.²² For models A and B, the structures of the $\text{Cu}_3(\mu\text{-pz})_3$ moiety are equilateral trigonal shape, and the $\mu_3\text{-X}$ are in the two capping positions of the trigonal–bipyramid. The five-coordinate Cu(II) atoms are in the distorted trigonal–bipyramidal environment. Experimentally, the $\mu_3\text{-halogen}$ singly bridged $\text{Cu}_3(\mu_3\text{-X})(\mu\text{-pz})_3\text{Cl}_3$ ($\text{X} = \text{Cl}$ and Br) complexes have not been synthesized. However, to investigate the significant influence of the Cu–($\mu_3\text{-X}$)–Cu angles on the magnetic properties of the trigonal trinuclear Cu(II) complexes, we theoretically built the $\mu_3\text{-halogen}$ singly bridged models C (Figure 2, left) and D (Figure 2, middle) according to the $\text{Cu}_3(\mu_3\text{-O})(\mu\text{-pz})_3\text{Cl}_3$ X-ray crystal structure.²³ The $\text{Cu}_3(\mu_3\text{-O})(\mu\text{-pz})_3\text{Cl}_3$ complex is named model E (Figure 2, right).

To explore the mechanism of the magnetic coupling interaction for the trinuclear Cu(II) complexes conveniently, we build three dynamic models [$\text{Cu}_3(\mu_3\text{-X})(\mu\text{-pz})_3\text{Cl}_3$] ($\text{X} = \text{Cl}$, Br , and O for models C, D, and E) (Scheme 1) by pulling the $\mu_3\text{-X}$ bridge away from the center of the Cu_3 triangle plane. This technique has been used successfully to explain the coupling

* Corresponding author. Tel: +86-531-88361398. Fax: +86-531-88564464. E-mail: cbliu@sdu.edu.cn.

[†] Institute of Theoretical Chemistry, Shandong University.

[‡] Shandong Jianzhu University.

[§] University of Jinan.

^{||} Key Laboratory of Colloid and Interface Chemistry, Shandong University.

[⊥] Present address: Heze University, Heze 274015, Shandong, P. R. China.

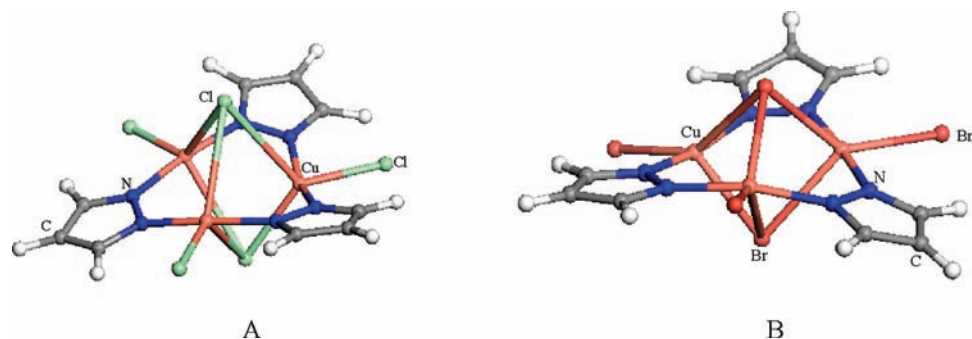


Figure 1. Structures of models A and B.

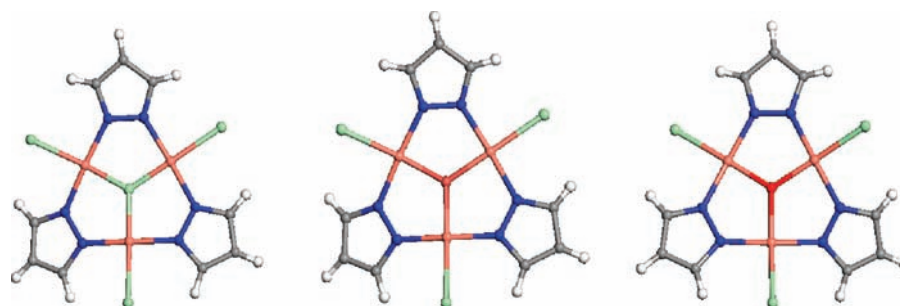
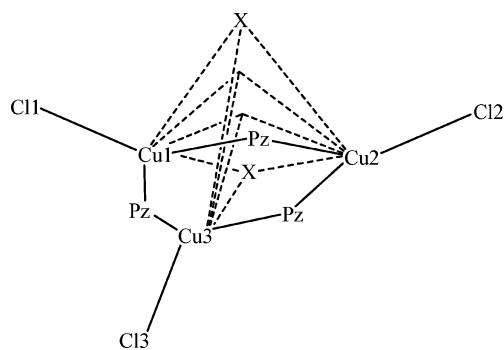
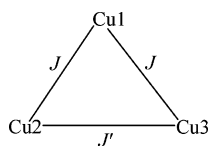


Figure 2. Primary structures for models C (left), D (middle), and E (right).

SCHEME 1: Dynamic Models of the μ_3 -X Singly Bridged Trinuclear Cu(II) Complexes (X = Cl, Br, and O for Models C, D, and E, Respectively; Pz = Pyrazolato Anion)



SCHEME 2: Primary Structure for Trigonal Symmetric Cu(II) Trimer



mechanism and magneto-structural correlation for the dinuclear transition-metal complexes.^{24,25} According to the experimental studies, the values of the Cu-(μ_3 -X)-Cu angle for the trinuclear Cu(II) complexes change in the range of 120–75°. Therefore, in these dynamic models, the Cu-(μ_3 -X)-Cu angles are changed from 120 to 76° by a step of 4° with the μ_3 -X ligands being pulled away from the Cu₃ plane, which is shown in Scheme 1.

3. Computational Details

For trigonal symmetric Cu(II) trimers, the primary structure is shown in Scheme 2. The spin Hamiltonian describing the low-lying states in zero field can be written as

$$\hat{H} = -2J(\hat{S}_{A_1}\hat{S}_B + \hat{S}_{A_2}\hat{S}_B) - 2J'\hat{S}_{A_1}\hat{S}_{A_2} \quad (1)$$

where J and J' denote the exchange coupling constants between adjacent copper ions (Scheme 1). Here the DFT-BS method proposed by Noodleman et al.^{26–28} is used to calculate the magnetic coupling constants.

Equation 1 can also be written as follows

$$\hat{H} = -J(\hat{S}^2 - \hat{S}_{A_1}^2 - \hat{S}_{A_2}^2 - \hat{S}_B^2) - (J' - J)(\hat{S}'^2 - \hat{S}_{A_1}^2 - \hat{S}_{A_2}^2) \quad (2)$$

where $\hat{S}' = \hat{S}_{A_1} + \hat{S}_{A_2}$, $\hat{S} = \hat{S}' + \hat{S}_B$. The relative energy of different spin states is

$$E(S, S') = -JS(S + 1) - (J' - J)S'(S + 1) \quad (3)$$

For these systems, $S_{A_1} = S_{A_2} = S_B = 1/2$, the level $E(1/2, 0)$ is taken as the energy origin. The relative energies of the states are

$$E_{BS2} - E_{BS1} = -J + J' \quad (5)$$

In this trigonal symmetry copper trimers system, we define three spin configurations with the following spin distributions: Cu1(\uparrow)-Cu2(\uparrow)-Cu3(\uparrow)(HS), Cu1(\downarrow)-Cu2(\uparrow)-Cu3(\uparrow)(BS1), and Cu1(\uparrow)-Cu2(\downarrow)-Cu3(\uparrow)(BS2). HS is the highest spin quartet state, which is an eigenstate of the spin operator \hat{S}^2 . BS1 and BS2 are broken symmetry states, which are the mixed state of eigenstates of the total spin operator \hat{S}^2 but not the pure eigenstates. As a result, we obtain the expression for J and J'

$$\begin{aligned}
 E\left(\frac{3}{2}, 1\right) &= -J - 2J' \\
 E\left(\frac{1}{2}, 1\right) &= 2J - 2J' \\
 E\left(\frac{1}{2}, 0\right) &= 0 \\
 E_{\text{HS}} - E_{\text{BS1}} &= -\frac{3}{2}J \quad (4)
 \end{aligned}$$

J and J' values are calculated using the broken symmetry approach under DFT framework. In our systems, J' is equal to J .

The calculations of magnetic constants are performed using the B3LYP, as implemented in Gaussian 03 code.²⁹ The initial guess for Gaussian is generated by the Jaguar 7.5,³⁰ which was successfully used to calculate the J of polynuclear transition-metal complexes by Ruiz et al.^{31,32} A basis set of TZV quality is used. The convergence criterion of SCF is 10^{-8} .

4. Results and Discussion

4.1. Elucidation on Magnetic Coupling Interaction Mechanism. As a significant factor to judge the magnetic properties of the molecular magnet, the magnetic coupling constant J is the bridge between the experimental and theoretical researches. Experimentally, the J values are obtained from the fitting of the experimental data. Theoretically, the J values can be calculated by the configuration interaction (CI) methodologies and the DFT-based methods.^{12,13} The CI methodologies can generate relatively accurate J values and effectively manipulate symmetry and spin-adapted eigenstates of the exact Hamiltonian, but their computational cost limits their application to large model systems.¹³ Moreover, DFT-based calculations are proven to be very reliable and convenient for the correlated materials from magnetic molecules to magnetic solids.^{8,33-36} Therefore, the DFT-BS method is used here to calculate the J values to elucidate the coupling interaction.

The calculated J values of the two μ_3 -X doubly bridged models A and B along with the experimental J values²² are summarized in Table 1. The calculated J values of models A and B are both positive ($J = 69.6 \text{ cm}^{-1}$ for model A and $J = 43.4 \text{ cm}^{-1}$ for model B), which is very consistent with the experimental results that there exists ferromagnetic interaction in models A and B and that the magnetic interaction in model A is stronger than that in model B.²² The calculated J for model E with $\text{Cu}-(\mu_3\text{-O})\text{-Cu} = 120^\circ$ is -989.8 cm^{-1} . This indicates that the magnetic interaction in the primary compounds is strong antiferromagnetic coupling, which is also in agreement with the experimental result ($J = -500 \text{ cm}^{-1}$).²³ The calculated J values are greater than the experimental results, and this maybe due to the modeling of the structures. Also, from Table 1, it is obvious that the magnetic properties of the models with different $\text{Cu}-(\mu_3\text{-X})\text{-Cu}$ angles are greatly different. To explain this significant difference, the magnetic mechanisms of the dynamic models C, D, and E are discussed in detail in the next sections.

TABLE 1: Calculated J Values of Models A and B

J/cm^{-1}	model A	model B
J_{exptl}	28.6 ^a	3.1 ^a
J_{calcd}	69.6	43.4

^a Reference.²²

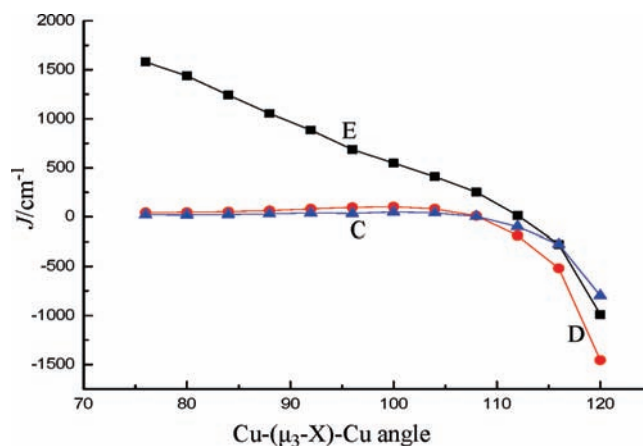


Figure 3. Plot of the J values versus the increasing $\text{Cu}-(\mu_3\text{-X})\text{-Cu}$ angles for the dynamic models C, D, and E ($X = \text{Cl}, \text{Br},$ and O for models C, D, and E, respectively).

4.2. Dependence of the Magnetic Coupling on the $\text{Cu}-(\mu_3\text{-X})\text{-Cu}$ Angles. To investigate the magneto-structural correlation, we also calculated the magnetic coupling constants J for the three dynamic models C, D, and E. The plots of J values versus the $\text{Cu}-(\mu_3\text{-X})\text{-Cu}$ angles are shown in Figure 3. Obviously, with the $\text{Cu}-(\mu_3\text{-X})\text{-Cu}$ angle changing from 76 to 120° , namely, the geometry of $\text{Cu}_3(\mu_3\text{-X})$ moiety changing from tetrahedron to equilateral triangle, the magnetic coupling constants J of the three models are decreasing from positive to negative. This indicates that the magnetic interactions of the three models are changed from ferromagnetic coupling to antiferromagnetic coupling. This variation trend is meaningful for designing the trinuclear $\text{Cu}(\text{II})$ complexes with the corresponding coupling interaction by changing the $\text{Cu}-(\mu_3\text{-X})\text{-Cu}$ angle.

According to Figure 3, the variation trends of curves C and D are very similar. With the $\text{Cu}-(\mu_3\text{-X})\text{-Cu}$ angles increasing from 76 to 100° , the J values of models C and D have a slight increase, and the J values begin to decrease with the $\text{Cu}-(\mu_3\text{-X})\text{-Cu}$ angles increasing from 100 to 120° . Significantly, at the point of $\text{Cu}-(\mu_3\text{-X})\text{-Cu} = 108^\circ$, the J values of models C and D change from positive to negative. In other words, the magnetic interactions of both models C and D are changed from ferromagnetic coupling to antiferromagnetic coupling at this point. It can be concluded that the halogen $\mu_3\text{-X}$ bridging ligands in the trinuclear $\text{Cu}(\text{II})$ complexes have similar behavior and influence on the magnetic coupling. However, the variation trend of the curve for model E is much different from that of models C and D. The J values of model E decrease in the whole range of the $\text{Cu}-(\mu_3\text{-O})\text{-Cu}$ angle (from 76 to 120°). Moreover, in the range of 76 to 108° , the variation value ΔJ as the $\text{Cu}-(\mu_3\text{-X})\text{-Cu}$ angle changing 4° for model E is about 180 cm^{-1} , which is much larger than the ΔJ (the maximum value is 70 cm^{-1}) for models C and D. This indicates that the magnetic properties of the trigonal trinuclear $\text{Cu}(\text{II})$ systems are much more sensitive to the oxygen bridging ligand than the halogen bridging ligand, which is in agreement with the results of the dinuclear $\text{Cu}(\text{II})$ complexes.⁸ At the point of $\text{Cu}-(\mu_3\text{-O})\text{-Cu} = 112^\circ$, the J value of model E changes from positive to negative. This suggests that the magnetic interaction of the $\mu_3\text{-O}$ bridged systems can be effectively controlled with changing the $\text{Cu}-(\mu_3\text{-O})\text{-Cu}$ angle.

4.3. Spin Distribution Analysis. To explain further the magnetic coupling mechanisms of the trigonal trinuclear systems, we analyze the spin density distribution. The calculated spin densities for quartet state on the $\text{Cu}(\text{II})$ centers and the ligand atoms versus the $\text{Cu}-(\mu_3\text{-X})\text{-Cu}$ angles are given in Figure

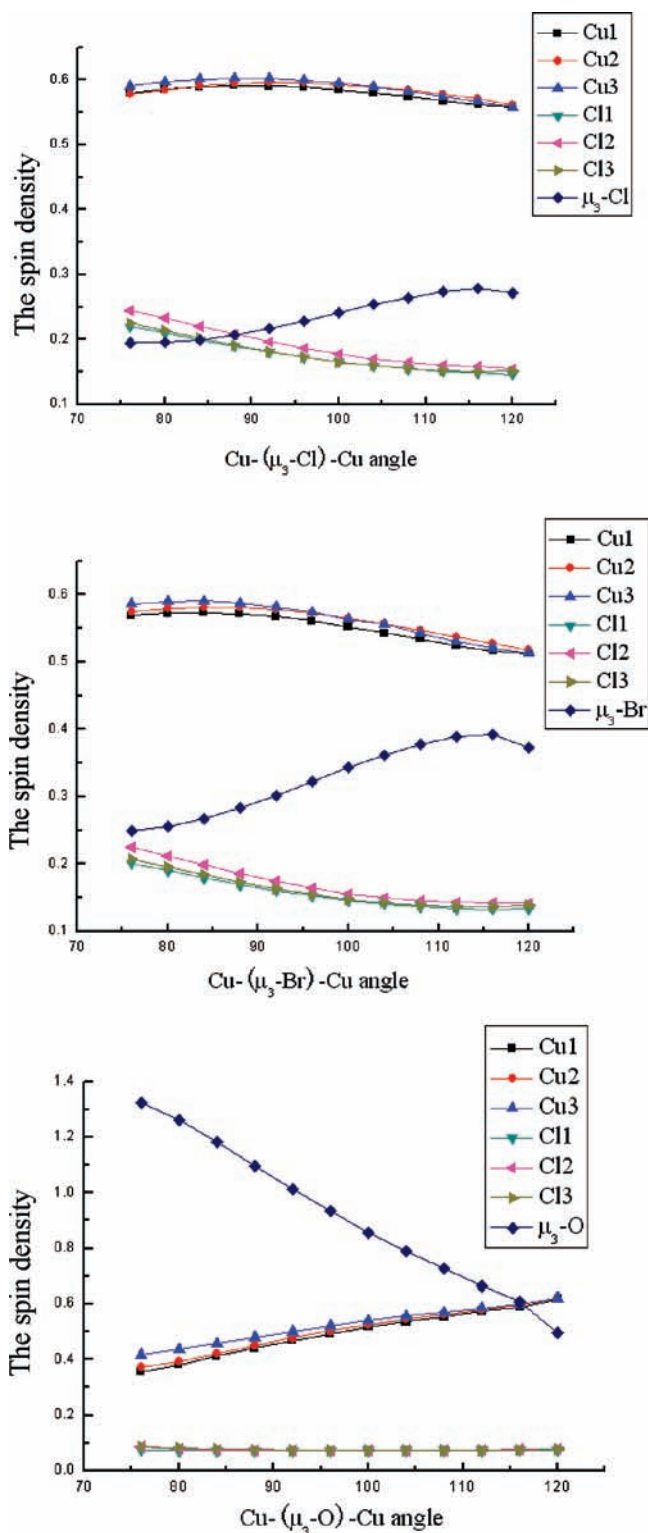


Figure 4. Plot of the spin population on the selected atoms versus the $\text{Cu}-(\mu_3\text{-X})\text{-Cu}$ angles for the high spin states of models C, D, and E.

4. For all of the models, the Cu(II) centers have the largest spin densities, and the spin densities on the terminal ligand atoms have the same sign (α spin) with the Cu(II) centers, which indicates that the spin delocalization has taken place from the Cu(II) centers to the coordinated ligand atoms. In general, the spin delocalization always results in the antiferromagnetic interaction, whereas the spin polarization leads to the ferromagnetic interaction. However, according to our research, in the trinuclear Cu(II) systems, the spin delocalization between

$\mu_3\text{-X}$ bridging ligand and the Cu(II) centers contributes to both ferromagnetic and antiferromagnetic coupling interactions.

With the increase in the $\text{Cu}-(\mu_3\text{-X})\text{-Cu}$ angles, the spin densities on the three Cu(II) centers decrease gradually in models C and D, whereas in model E, the spin densities on the Cu(II) centers increase smoothly. For the bridge $\mu_3\text{-X}$ atoms, the variation trend of spin densities on them is opposite to that on the Cu(II) centers. Moreover, the spin distribution variation on the terminal ligands is small. This result indicates that the unpaired electron is mainly transferred from the Cu(II) centers to the bridge ligand atoms.

In the $\text{Cu}-(\mu_3\text{-X})\text{-Cu}$ range of $76\text{--}100^\circ$, the spin densities on the Cu(II) centers for models C and D are mildly decreasing, which indicates that the spin delocalization becomes stronger, corresponding to the slightly increasing J values (Figure 3). For model E, the marked increasing spin densities on the Cu(II) centers correspond to the weak spin delocalization, and it may result in the greatly decreasing J value. Moreover, at the same angle, the spin densities on the Cu(II) centers of model E are much smaller than that of models C and D. For example, in the ground state, the spin density on Cu1 of model E is 0.3561 for $\text{Cu}-(\mu_3\text{-X})\text{-Cu} = 76^\circ$, whereas it is 0.5694 for model C and 0.5799 for model D. This suggests that the spin delocalization of the $\mu_3\text{-O}$ singly bridged model E is much greater than that of the $\mu_3\text{-halogen}$ singly ($\text{X} = \text{Cl}$ or Br) bridged models C and D. According to the calculated J values, the coupling interaction of model E is stronger than that of models C and D for $76 \leq \text{Cu}-(\mu_3\text{-X})\text{-Cu} \leq 100^\circ$. This suggests that the spin delocalization favors the ferromagnetic coupling interaction. From the above discussion, it can be concluded that the spin delocalization in the trigonal trinuclear Cu(II) complexes is not the criterion to judge the antiferromagnetic or ferromagnetic magnetic interaction.

4.4. Spin Frustration. Spin frustration could be easily pictured by a trigonal system connected by antiferromagnetic interaction. It could cause neighboring spin moments to prefer an antiparallel “up–down” spin arrangement. In this situation, any two spin moments could align antiparallel, but the third moment could not be antiparallel to its neighbors. Geometrically spin frustrated magnets usually consist of a macroscopic array of such trigonal units. Figure 5 shows the plots of the E/J' versus the ratio J/J' for trigonal symmetric system, where E denotes the energy of different spin states (J and J' , see Scheme 2). The exact nature of the ground states depends on the ratio J/J' . It is obvious that for the ferromagnetic coupling system (Figure 5, top), the ground state is high spin state $E(3/2,1)$. Therefore, despite the variation of the ratio J/J' , there is no spin frustration in these systems. In the antiferromagnetic coupling systems, J and J' are negative, and the ground state varies with the changing ratio J/J' (Figure 5, bottom). For $0 < J/J' < 1$, the ground state is $E(1/2,0)$, and for $J/J' > 1$, the ground state is $E(1/2,1)$. When J/J' is equal to 1, the ground state is accidentally degenerate, and the spins are unable to decide which state to stand in. Therefore, the system is shown to be frustrated. For the models we investigated, the J values are equal to the J' values. Therefore, there exists spin frustration phenomena when the coupling interaction is antiferromagnetic.

4.5. Molecular Orbital Analysis. Experimentally, each of the three Cu(II) centers exhibits a square-planar four-coordinate geometry. Therefore, it is obvious that the unpaired electrons of Cu(II) centers occupy the $d_{x^2-y^2}$ orbitals of models C, D, and E, which is in agreement with the calculated molecular orbital. For these molecular magnetisms, the orbitals located on the Cu(II) centers are defined as the local magnetic orbitals, whereas the singly occupied molecular orbitals in the high spin state

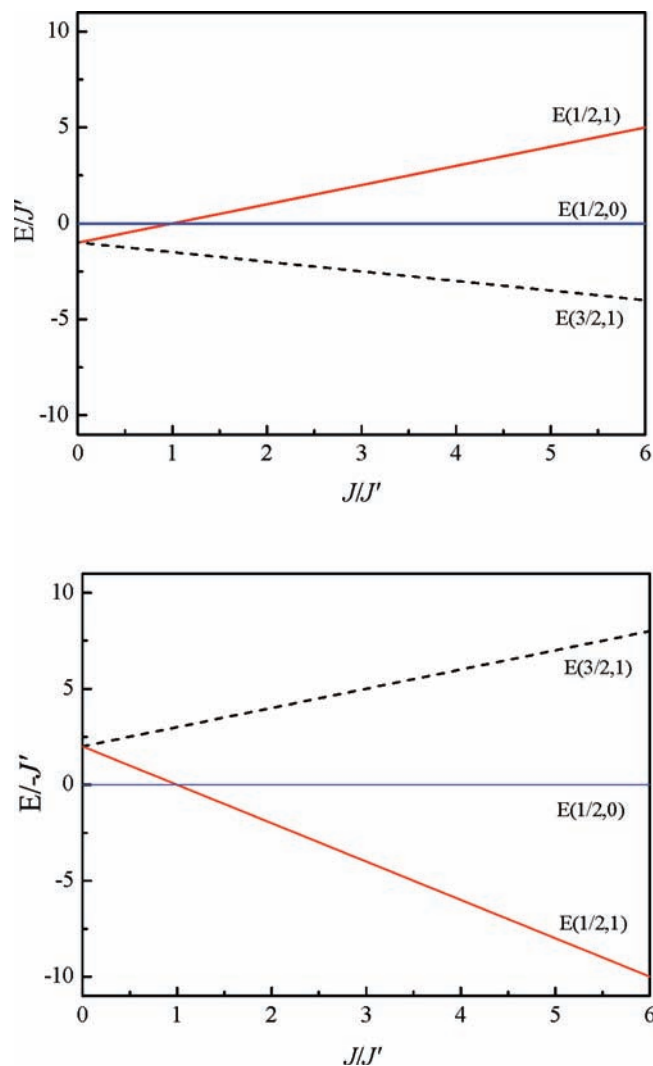


Figure 5. Variation of E/J' versus the ratio J/J' . (The top is the plot for the ferromagnetic system, and the bottom is the plot for the antiferromagnetic system.)

are regarded as molecular magnetic orbitals. Figure 6 gives the three singly occupied molecular magnetic orbitals (HOMO, HOMO-1, and HOMO-2) of each compound.

For models C, D, and E, the corresponding magnetic orbitals are much similar. Seen from the HOMO, the p orbitals of the μ_3 -X bridging ligands interact with the $d_{x^2-y^2}$ orbitals of Cu1 and Cu3 by the σ pathway, which is the most effective pathway to get the largest overlap of the orbitals. However, there is almost no interaction between the p orbitals of the μ_3 -X and the $d_{x^2-y^2}$ orbitals of Cu2. This interesting phenomenon is due to the spin frustration, which is resulted from the trigonal geometry of the compounds.

In addition, it is found that the larger the overlap between the p orbitals of the ligands and the $d_{x^2-y^2}$ orbitals of Cu(II), the stronger the antiferromagnetic coupling of the compounds. With the increase in the Cu-(μ_3 -X)-Cu angle, the overlap between the p orbitals of μ_3 -X and the $d_{x^2-y^2}$ orbitals of Cu(II) also increases. Therefore the ferromagnetic couplings for the models become weaker and weaker and are finally changed to be antiferromagnetic coupling. This result is consistent with the magneto-structural relationship analysis above. Therefore, the analysis of the molecular magnetic orbitals gives us a clear picture for the magnetic exchange characteristics and spin frustration phenomena in the studied molecules.

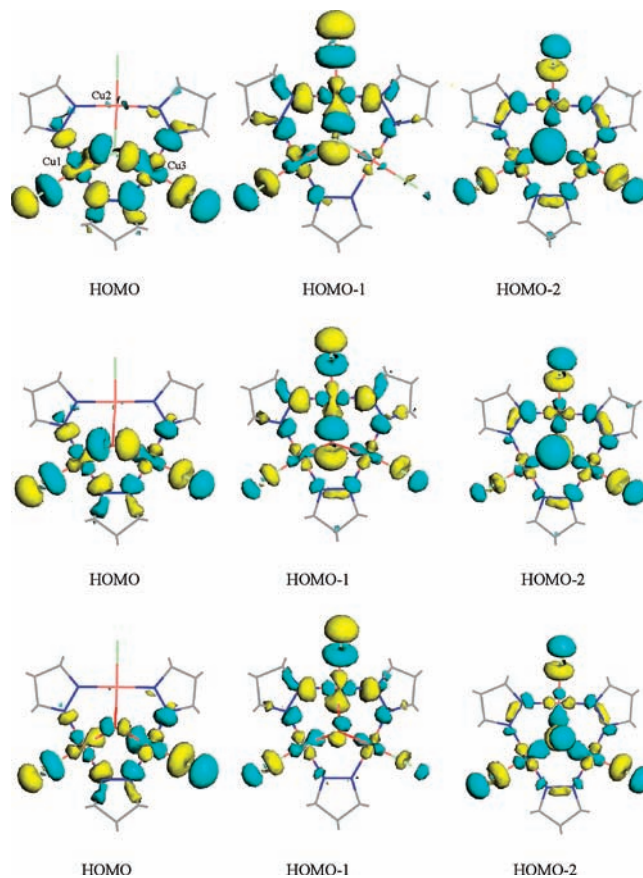


Figure 6. Diagrams of the magnetic orbitals of models C (top), D (middle), and E (bottom).

5. Conclusions

According to the DFT investigation, the magnetic interactions of trigonal trinuclear Cu(II) complexes are sensitive to the Cu-(μ_3 -X)-Cu angles. The magnetic coupling interaction is switched from ferromagnetic to antiferromagnetic as the Cu-(μ_3 -X)-Cu angle changing from 76 to 120°. The spin delocalization mechanism is reasonably used to explain the magnetic coupling for the trigonal trinuclear Cu(II) complexes. The variation of the J/J' ratio significantly affects the magnetic properties of the studied systems, which may adjust the magnetic properties of the system to synthesis novel molecule-based magnetic materials with desired magnetic function. The analysis of the molecular magnetic orbitals makes the magnetic exchange characteristic and spin frustration phenomena in the trigonal trinuclear Cu(II) complexes very visual.

Acknowledgment. This work is supported by the National Natural Science Foundation of China (nos. 20633060 and 20873075), the grant from the Major State Basic Research Development Programs (grant no. 2004CB719902), and the Project of Shandong Province Higher Educational Science and Technology Program. We also thank the Virtual Laboratory for Computational Chemistry of CNIC and Supercomputing Center of CNIC, Chinese Academy of Sciences. Special thanks to Prof. Eliseo Ruiz for helpful discussion.

Supporting Information Available: Energy values, values of S^2 , and geometrical parameters for the models. This material is available free of charge via the Internet at <http://pubs.acs.org>.

References and Notes

- (1) Spira-Solomon, D. J.; Allendorf, M. D.; Solomon, E. I. *J. Am. Chem. Soc.* **1986**, *108*, 5318.

- (2) Nguyen, H. T.; Shiemke, A. K.; Jacobs, S. J.; Hales, B. J.; Lidstrom, M. E.; Chan, S. I. *J. Biol. Chem.* **1994**, *269*, 14995.
- (3) Machonkin, T. E.; Solomon, E. I. *J. Am. Chem. Soc.* **2000**, *122*, 12547.
- (4) Epperson, J. D.; Ming, L. *J. Inorg. Biochem.* **2001**, *87*, 149.
- (5) Kim, Y.; Feng, X.; Lippard, S. J. *Inorg. Chem.* **2007**, *46*, 6099.
- (6) Faivre, D.; Schüler, D. *Chem. Rev.* **2008**, *108*, 4875.
- (7) Solomon, E. I.; Augustine, A. J.; Yoon, J. *Dalton Trans.* **2008**, 3921.
- (8) Kahn, O. *Molecular Magnetism*; VCH: New York, 1993.
- (9) Nie, H.; Aubin, S. M. J.; Mashuta, M. S.; Porter, R. A.; Richardson, J. F.; Hendrickson, D. N.; Buchanan, R. M. *Inorg. Chem.* **1996**, *35*, 3325.
- (10) Molenveld, P.; Engbersen, J. F. J.; Kooijman, H.; Spek, A. L.; Reinhoudt, D. N. *J. Am. Chem. Soc.* **1998**, *120*, 6726.
- (11) Tshuva, E. Y.; Lippard, S. J. *Chem. Rev.* **2004**, *104*, 987.
- (12) Yoon, J.; Solomon, E. I. *Coord. Chem. Rev.* **2007**, *251*, 379.
- (13) Le Guennic, B.; Robert, V. C. R. *Chimie* **2008**, *11*, 650.
- (14) Chandrasekhar, V.; Azhakar, R.; Senapati, T.; Thilagar, P.; Ghosh, S.; Verma, S.; Boomishankar, R.; Steiner, A.; Kogerler, P. *Dalton Trans.* **2008**, 1150.
- (15) Mitrikas, G.; Sanakis, Y.; Raptopoulou, C. P.; Kordas, G.; Pavassiliou, G. *Phys. Chem. Chem. Phys.* **2008**, *10*, 743.
- (16) van der Vlugt, J. I.; Demeshko, S.; Dechert, S.; Meyer, F. *Inorg. Chem.* **2008**, *47*, 1576.
- (17) Ramirez, A. P.; Espinosa, G. P.; Cooper, A. S. *Phys. Rev. Lett.* **1990**, *64*, 2070.
- (18) Bernhardt, P. V.; Sharpe, P. C. *J. Chem. Soc., Dalton Trans.* **1998**, 1087.
- (19) Wei, H. Y.; Hu, Z. C.; Chen, Z. D. *THEOCHEM* **2005**, *713*, 145.
- (20) Sarkar, B.; Ray, M. S.; Drew, M. G. B.; Figuerola, A.; Diaz, C.; Ghosh, A. *Polyhedron* **2006**, *25*, 3084.
- (21) Clegg, J. K.; Bray, D. J.; Gloe, K.; Gloe, K.; Jolliffe, K. A.; Lawrance, G. A.; Lindoy, L. F.; Meehane, G. V.; Wenzel, M. *Dalton Trans.* **2008**, 1331.
- (22) Boca, R.; Dihan, L.; Mezei, G.; Ortiz-Perez, T.; Raptis, R. G.; Telser, J. *Inorg. Chem.* **2003**, *42*, 5801.
- (23) Angaridis, P. A.; Baran, P.; Boca, R.; Cervantes-Lee, F.; Haase, W.; Mezei, G.; Raptis, R. G.; Werner, R. *Inorg. Chem.* **2002**, *41*, 2219.
- (24) Ren, Q. H.; Chen, Z. D.; Zhang, L. *Chem. Phys. Lett.* **2002**, *364*, 475.
- (25) Sun, Y. M.; Wang, L. L.; Wu, J. S. *Trans. Met. Chem.* **2008**, *33*, 1035.
- (26) Noodleman, L. *J. Chem. Phys.* **1981**, *74*, 5737.
- (27) Noodleman, L.; Davidson, E. R. *Chem. Phys.* **1986**, *109*, 131.
- (28) Noodleman, L.; Case, D. A. *Adv. Inorg. Chem.* **1992**, *38*, 423.
- (29) Frisch, M. J.; Trucks, G. W.; Schlegel, H. B.; Scuseria, G. E.; Robb, M. A.; Cheeseman, J. R.; Montgomery, J. A., Jr.; Vreven, T.; Kudin, K. N.; Burant, J. C.; Millam, J. M.; Iyengar, S. S.; Tomasi, J.; Barone, V.; Mennucci, B.; Cossi, M.; Scalmani, G.; Rega, N.; Petersson, G. A.; Nakatsuji, H.; Hada, M.; Ehara, M.; Toyota, K.; Fukuda, R.; Hasegawa, J.; Ishida, M.; Nakajima, T.; Honda, Y.; Kitao, O.; Nakai, H.; Klene, M.; Li, X.; Knox, J. E.; Hratchian, H. P.; Cross, J. B.; Bakken, V.; Adamo, C.; Jaramillo, J.; Gomperts, R.; Stratmann, R. E.; Yazyev, O.; Austin, A. J.; Cammi, R.; Pomelli, C.; Ochterski, J. W.; Ayala, P. Y.; Morokuma, K.; Voth, G. A.; Salvador, P.; Dannenberg, J. J.; Zakrzewski, V. G.; Dapprich, S.; Daniels, A. D.; Strain, M. C.; Farkas, O.; Malick, D. K.; Rabuck, A. D.; Raghavachari, K.; Foresman, J. B.; Ortiz, J. V.; Cui, Q.; Baboul, A. G.; Clifford, S.; Cioslowski, J.; Stefanov, B. B.; Liu, G.; Liashenko, A.; Piskorz, P.; Komaromi, I.; Martin, R. L.; Fox, D. J.; Keith, T.; Al-Laham, M. A.; Peng, C. Y.; Nanayakkara, A.; Challacombe, M.; Gill, P. M. W.; Johnson, B.; Chen, W.; Wong, M. W.; Gonzalez, C.; Pople, J. A. *Gaussian 03*, revision D.01; Gaussian, Inc.: Wallingford, CT, 2004.
- (30) *Jaguar*, version 7.5; Schrödinger, LLC: New York, 2008.
- (31) Ruiz, E.; Alvarez, S.; Cano, J.; Polo, V. *J. Chem. Phys.* **2005**, *123*, 164110.
- (32) Ruiz, E.; Cauchy, T.; Cano, J.; Costa, R.; Tercero, J.; Alvarez, S. *J. Am. Chem. Soc.* **2008**, *130*, 7420.
- (33) Cano, J.; Cauchy, T.; Ruiz, E.; Milios, C. J.; Stoumpos, C. C.; Stamatatos, Th. C.; Perlepes, S. P.; Christou, G.; Brechin, E. K. *Dalton Trans.* **2008**, 234.
- (34) Zein, S.; Borshch, S. A. *J. Am. Chem. Soc.* **2005**, *127*, 16197.
- (35) Wang, L. L.; Sun, Y. M.; Qi, Z. N.; Liu, C. B. *J. Phys. Chem. A* **2008**, *112*, 8418.
- (36) Hou, C.; Shi, J. M.; Sun, Y. M.; Shi, W.; Cheng, P.; Liu, L. D. *Dalton Trans.* **2008**, 5970.

JP9045897